Geomechanics and Engineering, *Vol. 31, No. 5 (2022) 461-476*
https://doi.org/10.12989/gae.2022.31.5.461

Scale effects on triaxial peak and residual strength of granite and preliminary PFC3D models

Xian Estévez-Ventosa[1], Uxía Castro-Filgueira[1], Manuel A. González-Fernández[1], Fernando García-Bastante[1], Diego Mas-Ivars[2,3] and Leandro R. Alejano*[1]

[1]*CINTECX, GESSMin group, Department of Natural Resources and Environmental Engineering, University of Vigo, Campus Lagoas, Vigo, Pontevedra, 36.310, Spain*
[2]*Swedish Nuclear Fuel and Waste Management Company (SKB), Evenemangsgatan 13, Box 3091, SE-169 03 Solna, Stockholm, Sweden*
[3]*Division of Soil and Rock Mechanics, Royal Institute of Technology (KTH), Brinellvägen 23, 100 44 Stockholm, Sweden*

(*Received November 10, 2021, Revised November 12, 2022, Accepted November 15, 2022*)

Abstract. Research studies on the scale effect on triaxial strength of intact rocks are scarce, being more common those in uniaxial strength. In this paper, the authors present and briefly interpret the peak and residual strength trends on a series of triaxial tests on different size specimens (30 mm to 84 mm diameter) of an intact granitic rock at confinements ranging from 0 to 15 MPa. Peak strength tends to grow from smaller to standard-size samples (54 mm) and then diminishes for larger values at low confinement. However, a slight change in strength is observed at higher confinements. Residual strength is observed to be much less size-dependent. Additionally, this study introduces preliminary modelling approaches of these laboratory observations with the help of three-dimensional particle flow code (PFC3D) simulations based on bonded particle models (BPM). Based on previous studies, two modelling approaches have been followed. In the first one, the maximum and minimum particle diameter (D_{max} and D_{min}) are kept constant irrespective of the sample size, whereas in the second one, the resolution (number of particles within the sample or ϕ_v) was kept constant. Neither of these approaches properly represent the observations in actual laboratory tests, even if both of them show some interesting capabilities reported in this document. Eventually, some suggestions are provided to proceed towards improving modelling approaches to represent observed scale effects.

Keywords: flat joint; Hoek-Brown criterion; intact granite samples; numerical methods; PFC; size effects

1. Introduction

This study advances towards a better understanding of scale effects in the triaxial strength of rock samples and investigates modelling approaches to represent the observed behavior. It is based on a complete series of triaxial strength laboratory tests on different-size granite samples and its interpretation in line with previous studies (Gonzalez-Fernandez *et al.* 2021), on the one hand. On the other, the authors present the development of 3D numerical models to reproduce these test results. Typically, previous research has addressed either laboratory tests and interpretation, or modelling. This study makes the effort of constructing comprehensive modelling approaches starting from test results and identifying relevant issues all along the processes of model building, calibration and results interpretation.

A good number of rock mechanics laboratory studies have addressed scale effects on unconfined rock strength (Bieniawski 1967, Pratt *et al*. 1972, Hoek and Brown 1980, Brace 1981, Price 1986, Pinto da Cunha 1990, Yoshinaka *et al.* 2008, Masoumi 2013, Quiñones *et al*. 2017), but only a few have focused on triaxial strength (Hunt *et al.* 1973, Walton 2018). Indeed scale effects on triaxial tests are still not clearly understood. The reason behind this can be the scarce triaxial laboratory tests at different scale as reported by various authors (Brace 1981, Masoumi *et al.* 2016).

Seminal scale effect studies on unconfined tests, such as that by Hoek and Brown (1980) observed a diminishing strength with sample size starting form standard size samples (54 mm diameter). This observation was generally confirmed in other studies for various types of rocks (Yoshinaka *et al.* 2008). Later, other studies (Masoumi *et al.* 2015, Quiñones *et al.* 2017) noted that for smaller rock specimens of intact rock from 15 mm to about 45 to 54 mm, UCS tend to be more variable and to increase in average, achieving a maximum value of UCS for the standard lab sample size.

Only a few studies have addressed scale effects on triaxial strength and those studies are rather limited. Among these, Walton (2018) mentioned that scale effects are not so apparent for triaxial cases than for uniaxial ones. Habib and Vouille (1966) pointed out that scale effects were less relevant for high confinement levels. There is a clear need of further experimental evidence and research on these topics.

With the aim of advancing in this knowledge, this study reviews a complete series of triaxial compressive tests in different size granite samples and the basic interpretation provided. Then, and building on previous developments of standard size samples (Castro Filgueira *et al.* 2016, 2017), the authors develop modelling approaches of these tests

*Corresponding author, Professor
E-mail: alejano@uvigo.es

ISSN: 2005-307X (Print), 2092-6219 (Online)

based on a particle flow code, in particular with BPM models made with PFC3D in line with Zhou *et al*. (2018); Ajamzadeh *et al*. (2018) or Xu *et al*. (2020). Problems faced when selecting model strategies to simulate different size samples are highlighted and discussed.

2. Scale effects on triaxial strength

Rocks are heterogeneous and variable natural materials, so their mechanical behavior is often difficult to understand and model both at micro and macroscopic levels. Some authors attribute these characteristics to rock formation and evolution associated to geological conditions, tectonic and weathering effects. Due to this generally complex nature, the mechanical behavior of a rock specimen, which is being loaded or deformed, depends on the volume of the sample tested. So, we can assume that rock strength may show significant scale effects. This topic is still not completely well understood, but these effects widely appear in rock mechanics when characterizing and determining properties of rock, joints or rock masses.

Pinto da Cunha (1990) mentioned the three main different causes for the variation of mechanical parameters in rocks and rock masses associated to scale. The first one is the effect related with jointing, representative of the rock masses. The second is the shape effect (Obert and Duval, 1967, Tuncay and Hasancebi 2009), caused by changing the specimen geometry, usually the slenderness. In this line, the ISRM (2007) suggested methods recommend a height-to-diameter ratio should of at least 2. Finally, Pinto da Cunha (1990) recognized other size-effects not related to the geometry or jointing, but just to sample size.

2.1 Studies on scale effects on uniaxial compressive strength

Several authors, Bieniawski (1967), for cubic coal samples, Pratt *et al*. (1972), Hoek and Brown (1980) and Price (1986) for cylindrical specimens, were among the first to study strength scale effects on UCS tests. Recently, new studies performed by several authors deepen on scale effects (Yoshinaka *et al*. 2008, Martin *et al*. 2014, Haeri *et al*. 2018a, b). These studies show that scale effects vary according to rock type, texture, micro-flaw occurrence and the level of alteration or weathering of the sample. All these studies suggest strength decreases when sample size increases, according to the so-called weak-link theory Weibull (1939). On the other hand, Massoumi (2013) and Quiñones (2017) found that the behavior of the smaller samples (less than 50 mm diameter) do not follow the established model, where strength decreases with size. This effect is thought to be related to the presence of large grain sizes in relation to sample size, so failure mechanisms can be associated to one single mineral grain or one single contact between grains.

2.2 Studies on scale effects on triaxial strength

Confinement relevantly affects rock behavior, so it should be considered when analyzing strength (Hoek and Brown 1980, Fan *et al*. 2019). Several studies have been performed on scale effects in UCS tests, this effect has been little studied in triaxial tests. Hunt *et al*. (1973) performed some tests in gypsum samples and Medhurst and Brown (1998) studied the triaxial behavior on coal. Being these very particular sedimentary rocks, their behavior may not represent properly that of granitic rocks. Only a few studies have been carried out in sandstone by Masoumi (2013) and in granite samples by Walton (2018), carrying out triaxial tests at different scales. These seminal studies report that strength tend to grow with sample size for 15- to 50-mm diameter specimens but then reduce its values when the size increase from this threshold size, according to the weak-link theory. In what concerns residual strength, a scarce number of studies on size dependency are found in literature (Masoumi 2013, Walton 2018). Although based on a limited number of tests, they suggest no notable trends of residual strength as a function of scale.

3. Results of peak and residual triaxial strength of Blanco Mera granite samples

To collect a representative number of data, the authors carried out a laboratory program for four different sample sizes of Blanco Mera granite (Gónzalez-Fernández *et al.* 2021, Alejano *et al*. 2021). This is a granite from NW of Spain well characterized in the literature (Arzúa and Alejano 2013). The grain distribution is scattered and the grain size typically varies from 1 to 6 mm for quartz and from 1 to 3 mm for feldspars, with smaller micas. A general good knowledge of the basic rock mechanics parameters of this granite is available (Arzúa and Alejano 2013, Alejano *et al.* 2017).

The sample diameters chosen for the testing program were 30, 38, 54 and 84 mm: see Fig. 1(a). For each diameter, around 30 samples were obtained for testing with a length-to-diameter ratio of at least 2. Standard triaxial tests were carried out for each group. For each sample size, typically 2 to 4 triaxial tests were performed for confinements between 0.2 and 15 MPa, with 2.5-MPa intervals. The authors performed about 25 triaxial strength tests for each sample size, including straining it until achieving a residual state. Hoek's cells and the corresponding sleeves for the larger size were manufactured specifically for the study: see Fig. 1(a).

3.1 Laboratory set up

A 2,000 kN press framework was used for testing: see Fig. 1(b) equipped with load cells and different strain measurement systems. The press is servo-controlled, a capability used to control test velocity. A dedicated software collects data while testing in terms of confinement, load and strains. To record strains, four gauges (two glued vertically and two diametrically were used). For further analysis of deformation after specimen failure, the volume displaced out of the Hoek's cell was also recorded. Unloading and loading cycles were performed, for possible further analysis in the post-peak phase. For the purposes of this study, peak

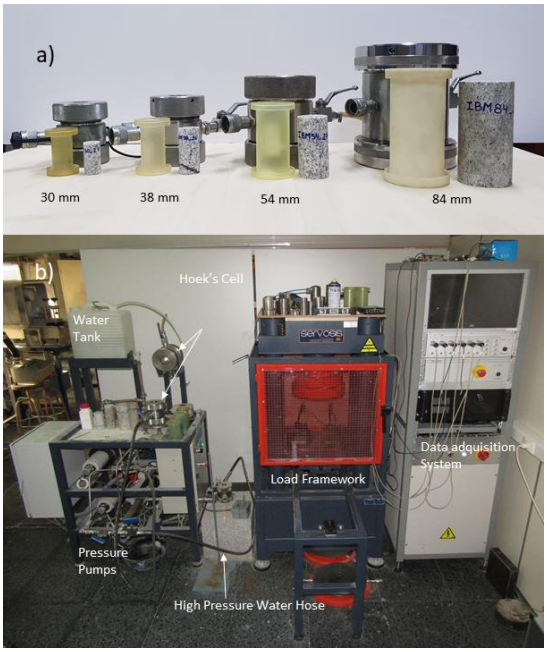

Fig. 1 (a) Different size specimens, sleeves and Hoek's cells to be tested and (b) Testing system and associated elements

Table 1 Mean results for each specimen size and confinement, for both peak and residual strengths, together with the coefficient of variation (CV)

Specimen diameter [mm]	σ_3 [MPa]	σ_1^{peak} [MPa]		σ_1^{res} [MPa]	
		Mean	CV	Mean.	CV
30	0.2	95.41	14.20	12.50	20.13
	2.5	117.69	36.19	25.50	25.50
	5.0	170.99	12.39	43.75	11.71
	7.5	176.58	27.22	59.67	42.08
	10.0	231.62	8.23	70.50	17.89
	12.5	255.68	10.76	75.50	2.81
	15.0	294.77	2.79	86.25	14.77
38	0.2	119.90	5.30	14.75	3.39
	2.5	156.82	8.41	28.33	21.57
	5.0	184.36	11.51	45.75	23.36
	7.5	208.87	19.50	58.00	26.09
	10.0	243.72	2.77	67.25	17.86
	12.5	280.84	2.88	77.67	6.48
	15.0	293.56	2.40	89.75	6.89
54	0.2	131.27	13.24	21.13	50.26
	2.5	173.82	16.06	34.67	16.40
	5.0	164.38	9.87	49.75	37.97
	7.5	215.81	12.96	56.00	12.88
	10.0	235.14	10.87	64.25	10.58
	12.5	260.07	4.16	70.00	10.10
	15.0	278.08	14.52	87.50	11.22
84	0.2	85.81	28.36	8.75	41.07
	2.5	142.46	11.28	29.00	9.12
	5.0	163.57	10.44	45.00	20.04
	7.5	213.77	11.82	60.33	17.88
	10.0	216.39	8.76	66.00	17.19
	12.5	239.77	7.42	77.33	14.24
	15.0	278.55	9.75	88.25	3.86

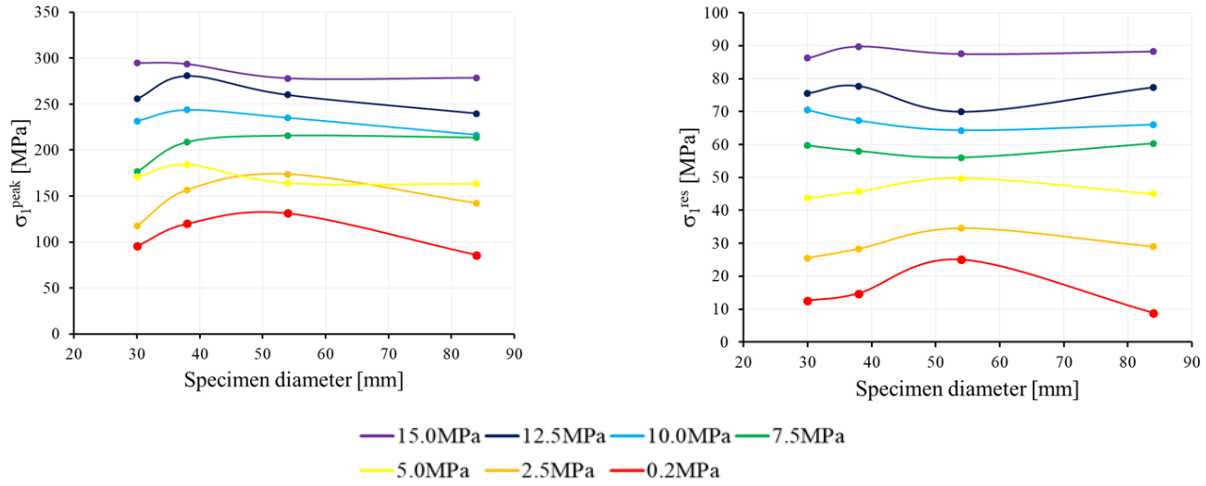

(a) (b)

Fig. 2 Mean results for each specimen confinement graphed against size: (a) peak strength and (b) residual strength

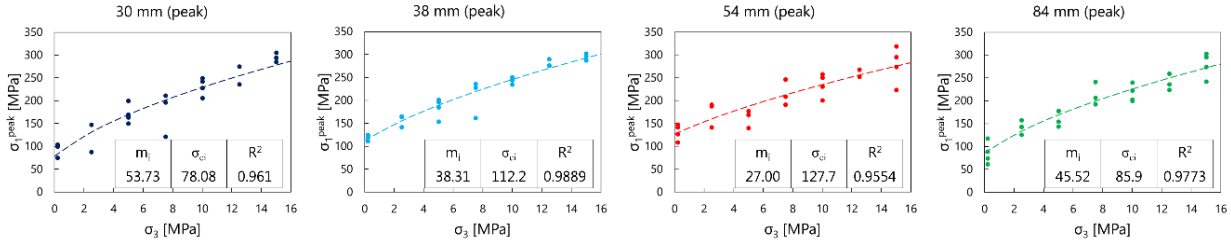

Fig. 3 Representation of peak strengths together with Hoek-Brown fits for each specimen size

and residual strengths were computed and analyzed in relation with the specimen size.

3.2 Studies on scale effects on triaxial strength

Both average peak and residual strength average values are shown in Table 1, together with their coefficients of variation (standard deviation over mean) for the 97 tests.

Peak strength results (Gonzalez-Fernandez *et al.* 2021), were published with a preliminary interpretation, showing that scale effects are relevant at low confinement, but milder for higher confinements in line with Habib and Vouille (1966). Residual strength results were interpreted within a broad data base of residual response of granitic rocks by Alejano *et al.* (2021), concluding that residual strength appears to be independent of specimen size, particularly at high stresses in line with other published studies (Gao and Kang 2016).

3.3 General trends

The Hoek-Brown failure criteria is typically used to represent strength in rock and rock masses (Hoek and Brown 1997, Ranjbarnia *et al.* 2020, Chinaiei *et al.* 2021), so it is also used in this study. The peak strength results, are interpreted regarding scale and confinement. In Fig. 2 the values of mean peak and residual strengths for different confinements are graphed against sample size. Peak and residual strength grows with confinement as expected (Fig. 2). A special case happens in strength peak values at 2.5 and 5 MPa, where both of the curves crosses, something that can be attributed to the natural variability of the rock.

The double scale size effect (Masoumi 2013) is clearly identified for low confinement levels. This means that strength grows from smaller samples (30 mm diameter) to mid-size samples in the range 45-55 mm diameter (NX or 54 mm diameter in this case) and then it mildly decreases for larger samples (84 mm diameter). This phenomenon is clearly observed for low confinement tests (0.2-5 MPa), but not so clearly marked for higher confinements (10-15 MPa).

To compile results, the Hoek-Brown failure criterion was fit to strength results for every size group. Hoek-Brown parameters σ_{ci} and m_i, are obtained by fitting the basic Hoek-Brown equation (Hoek *et al.* 2002)

$$\sigma_1 = \sigma_3 + \sigma_{ci}\left(\frac{m_i}{\sigma_{ci}}\sigma_3 + 1\right)^{0.5} \quad (1)$$

To do this fitting we resort to the Matlab application Curve Fitting tool, which fits the results to Eq. (1) by iterating the m_i and σ_{ci} values. This tool minimizes the non-linear least square error by comparing the results. It should be noted that value of Hoek-Brown *s* parameter for intact rock is equal to 1. The results of the fits, including the parameters and coefficients of determination, together with the laboratory results data, represented in Hoek-Brown axes, are presented in Fig. 3 for every specimen size.

It should be noted that the values of the m_i and σ_{ci} here

Table 2 Hoek-Brown parameters obtained for residual strengths

H-B parameter	30 mm	38 mm	54 mm	84 mm
m	53.73	38.31	27	45.52
σ_{ci} [MPa]	78.08	112.2	127.7	85.9
GSI	29.77	30.77	35.41	32.28
R^2	0.985	0.9863	0.8638	0.9959

obtained slightly differ from those showed in Gonzalez-Fernandez *et al.* (2021), where they were obtained by fitting a line to the transformed data set.

As it is observed in Fig. 3, the computed σ_{ci} follows the same trend as that observed for peak strength in 0.2 MPa and for other strength studies (Quiñones *et al.* 2017), it grows from 30 mm to 54 mm and then it decreases in 84 mm. Also for high confinements, the values of the fit have more or less the same trend, but not so marked. Regarding the m_i parameter, it follows an opposite trend with respect to the uniaxial compressive strength. It has a high value for 30 mm samples (m_i = 53.73), then it decreases for 38 mm samples (m_i =38.31), continue to decrease for 54 mm (m_i =27) and then grows again in 84 mm (m_i =45.52).

For residual strength, the generalized Hoek-Brown criterion for rock masses (Hoek *et al.* 2002) is fit

$$\sigma_1 = \sigma_3 + \sigma_{ci}\left(m_b\frac{\sigma_3}{\sigma_{ci}} + s\right)^a \quad (2)$$

$$m_b = m_i exp\left(\frac{GSI - 100}{28 - 14D}\right) \quad (3)$$

$$s = exp = \left(\frac{GSI - 100}{9 - 3D}\right) \quad (4)$$

$$a = \frac{1}{2} + \frac{1}{6}\left(exp\left(\frac{-GSI}{15}\right) - exp\left(\frac{-20}{3}\right)\right) \quad (5)$$

This criterion is more suitable to assess the residual strength because it encompasses the geological strength index (GSI), an index of the rock mass quality, related to the jointing or fracturing level of the rock mass or of the broken material, such as in this case. Accordingly, the generalized H-B criterion is used to fit the residual strength data instead of the basic H-B criterion (Hoek *et al.* 1995), more suitable for intact rocks.

To compute and obtain the values of the parameters for the generalized H-B criterion, *GSI*, m_b, *s* and *a*, it was used the same method as in H-B criterion. In this case, the Eqs. (3)-(5) were cleared on the Eq. (2), and using the parameters of the H-B criterion calculated before, we have a GSI dependent equation.

The results of the values of the *GSI* and the coefficients of determination (R^2) are presented in Table 2, showing that the *GSI* residual values are sensibly constant and ranging from 30 to 35 in line with Alejano *et al.* (2021). These values would correspond to those found in nature for a fractured rock mass, according to the *GSI* classification. The coefficients of determination (R^2) are very close to one for 30, 38 and 84 mm. For the 54 mm case, R^2 is slightly smaller, something attributed to rock variability, but it is large enough to ensure that the *GSI* value correlates reasonably well with the obtained lab residual data.

4. PFC modelling of granite samples

With the objective of trying to improve our modelling capabilities and also aiming to understand how scale effects affect particle model simulation results, numerical modelling simulations of the presented tests with PFC3D were devised and carried out following previous works with standard size sample models (Castro-Filgueira *et al.* 2016, 2017, 2020). The basic idea was to analyse the role of scale in these particle simulations, in line with other studies (Haeri *et al.* 2018a, c).

PFC3D is a distinct element program, where a model simulates the movement and interaction of finite-sized particles, which are rigid bodies that interact at pair-wise contacts (Itasca 2019). Previous mechanical behavior models of intact rock samples carried out by different authors (Potyondy 2015, Hazzard *et al.* 2000, Cho *et al.* 2007, Shöpfer *et al.* 2009) showed the interest of the approach and reasonable reliability of the PFC models in order to simulate the rock behavior by means of BPM (Bonded Particle Models). In particular, the flat-joint models proofed their capability to reproduce the increase on strength of rock sample in relation to confinement (Potyondy 2018, Wu and Xu 2016, Yang *et al.* 2019, or Peng *et al.* 2017), something that previous models were not able to achieve.

4.1 PFC modelling of specimens

Some numerical studies were developed in the past by part of the authors of this paper to numerically model the behavior of Blanco Mera granite by means of particle models. To develop this investigation, the PFC3D software was selected, starting with available parallel-bond contact models of intact rock samples that provided results published in Castro-Filgueira *et al.* (2016). Despite the fact that the parallel-bond contact model can simulate rocks, some deficiencies were observed to mimic the actual triaxial strength behavior of a hard rocks like granite.

The parallel-bond contact model provides the mechanical behavior of a cement that establish an elastic interaction between the particles and transmit both forces and moments between the grains (Potyondy 2015). When this cement breaks, it is removed and it does not provide resistance to rotation anymore: see Fig. 4(a), which avoids an appropriate representation of the frictional behavior of rock (Wu and Xu 2016). However, in the flat-joint contact, the grains have faces, drawn as spherical cores with skirted faces, so the interface is discretized into elements that can be bonded or unbonded: see Fig. 4(b) (Potyondy 2015). Accordingly, even an interface completely broken still resists relative rotations. Due to the resistance to rotations after bond breakage, this contact model

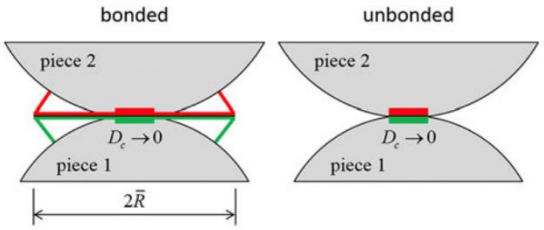

a) Parallel-bond contact

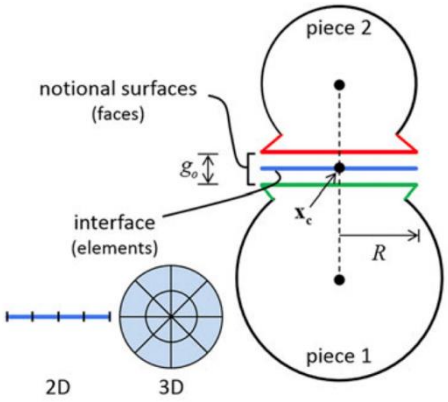

b) Flat-joint contact

Fig. 4 (a) Parallel-bond contact before (left) and after (right) bond breakage and (b) Flat-joint contact. Both according to Potyondy (2015)

better simulates the frictional and post-failure behavior of hard rocks like the Blanco Mera granite (Castro-Filgueira *et al.* 2017, Li *et al.* 2018).

Consequently, after the first studies, the contact model was updated to the more evolved and accurate flat-joint contact model. For this case, the number of micro-parameters to be calibrated is higher, so the calibration procedure –that is an oriented trial-and-error process– is time consuming. In order to reduce this time, a sensitivity analysis approach of the micro-parameters was carried out that simplified the calibration process (Castro-Filgueira *et al.* (2017), where the authors found out some influence of strength and stiffness micro-parameters on macro-properties, that help to guide the calibration process.

In order to reduce the total number of calibration simulations to perform, Coetzee (2017) proposed a comprehensive calibration procedure by performing simulations of loose granular materials in a specific order to isolate certain parameters, starting from particle size and distribution, then particle density, followed by contact friction and particle stiffness.

In particular, the micro-properties of the intact rock and joints in the studied samples are chosen via such a calibration process by matching laboratory test results (intact rock uniaxial and compressive strength, Young's modulus, Poisson's ratio and post-failure trends) following the procedures outlined by Potyondy and Cundall (2004) and further developed by Mas-Ivars *et al.* (2013) for the case of rock.

This approach was followed by the authors (Castro-Filgueira *et al.* 2017), in combination with suggestions on micro-parameters by Wu and Xu (2016) for a first calibration and a sensitivity analysis focusing granitic rock, which was carried out to reflect the influence of relevant inputs on controlled outputs.

Note that in the presented simulations, the elastic, uniaxial and triaxial strength and post-failure response are considered for different scales, unlike in many published simpler studies where only elastic or elastic and uniaxial strength (Yoon 2007, Ding *et al.* 2014) are considered for one sample size, so the level of accuracy is logically smaller. However, identified trends are relevant in order to advance towards more realistic models, particularly those accounting for scale.

A basic problem of models resorting to parallel-bond contacts was identified when carrying out first simulations of rocks with particle flow codes, associated to a low value of friction. This produced low macroscopic friction values, low unconfined compressive strength to tensile strength ratios (UCS/UTS) and linear strength envelopes with low *m* values (Wu and Xu 2016, Castro-Filgueira *et al.* 2017). The flat joint contact model (Potyondy 2018) was developed to overcome these problems partially associated to the use of parallel bond model and several authors show that it can better represent rock strength response (Wu and Xu 2016, Li *et al.* 2018).

Li *et al.* (2018) propose a calibration procedure to calibrate the micro-parameters for the flat-joint model for both uniaxial compression and tensile test simulations accounting for model size and resolution. The findings in Li *et al.* (2018) are in line with some results of this study. However, they do neither consider triaxial compression do nor analyze post-failure behavior trends.

Table 3 Micro-parameters of the flat-joint model calibrated to obtain the Blanco Mera granite response (from Castro-Filgueira *et al.* 2020)

Packing		Linear model		Flat-joint model	
Parameter	Value	Parameter	Value	Parameter	Value
ρ [kg/m^3]	2600	E_n* [GPa]	53	E* [GPa]	53
D_{max}/D_{min}	1.66	K_n	1.7	K	1.7
g_0 [mm]	0.5	μ_n	0.5	σ_{t_c} [MPa]	4±20%
N_α	3			c [MPa]	132±20%
N_r	1			ϕ (º)	47
ϕ_B	1			μ_n	0.5
ϕ_G	0				
E_b* [GPa]	79.5				
P_m [kPa]	100				

Table 4 Peak and residual strength results for intact rocks tested in laboratory vs PFC simulations (modified from Castro-Filgueira 2020)

σ_3 [MPa]	σ_1^{peak} [MPa]		σ_1^{res} [MPa]	
	Laboratory	PFC	Laboratory	PFC
UCS	109.21	124.25	-	-
2	180.18	180.40	36.50	24.55
4	210.07	211.96	48.50	33.90
6	230.58	236.48	65.00	51.38
10	265.88	278.52	91.75	97.43
12	299.71	297.54	97.00	126.69
14	311.62	317.01	180.00	154.27

Various authors have advanced towards artificial intelligent (AI) based techniques in order to improve calibration procedures, for instance Kim *et al.* (2021), Xu *et al.* (2021) or De Simone *et al.* (2019) focusing the Elastic Young's moduli and the UCS in a micro-mechanical model approach. Similar AI-based approaches were tested to other numerical modelling techniques (Miranda *et al.* 2010, 2011), but they tend to suffer from the same limitations. Indeed, while these methods are promising, they usually address a limited number of output parameters, and they found difficulties when trying to reflect the whole behavior of rock in terms of elasticity, unconfined and triaxial compressive strength and post-failure behavior trends, as the study presented here.

Finally, taking into account this study, the calibration of the granite with the flat-joint contact model was done. The obtained values of the micro-parameters are presented in Table 3, which have been recently published in a study (Castro-Filgueira *et al.* 2020), where the models of intact rock were extended to the behavior of artificially fissured samples. These micro-properties presented in Table 3 are the ones used for all the models carried out for this study. Additionally, differences arise between the previous study and the present one in that the version of the software was PFC 5.0 for the former and PFC 6.0 for this one.

4.2 Previous strength results on standard size samples

After calibrating the models, uniaxial and triaxial tests on intact and fissured specimens were conducted (Castro-Filgueira *et al.* 2020). The obtained results for intact specimens are shown in Table 4. The procedure to obtain the strength parameters was the same as that carried out in laboratory, including previous confinement of the sample and then loading the specimens at a constant strain rate.

The results analyzed here includes peak strength (σ_1^{peak}), which is taken as the maximum axial strength observed in the test, and residual strength (σ_1^{res}) normally coincident with the occurrence of a strength plateau in the stress-strain curve.

To compute this value of residual strength at this plateau, the end of compression test is controlled by the so-called load-termination factor, a constant that multiplied by the expected peak strength provides an estimate of the estimated range of residual strength. This parameter was calibrated test-by-test, getting a range from 0.02 –for lower confinements and specimen diameters, where rock behaves more fragile– to 0.10 –for higher confinements and diameters, where rock is harder–. These values imply higher simulation times, around 6-8 hours each, but it allows to get the complete stress-strain curve in a conservative way. It is relevant to mention that the load-termination factor values used cannot necessarily be generalized to study other rocks and it should be fine-tuned according to the given confinement range, even if they can be roughly indicative for hard rock PFC3D models.

The indicated updated tests results in terms of peak and residual strength for standard size samples are presented together with laboratory averages in Table 4.

The peak strength results obtained from the PFC simulations reasonably fit the laboratory ones. When no confinement is applied (*UCS*), the higher difference in the results is observed, but generally the found differences are lower than the natural variability of the rock observed at laboratory scale. Regarding the residual strength, more variability is observed in the laboratory and test results. The authors consider that the general trends are reasonable well reflected, but they also recognize there is further room for improvement.

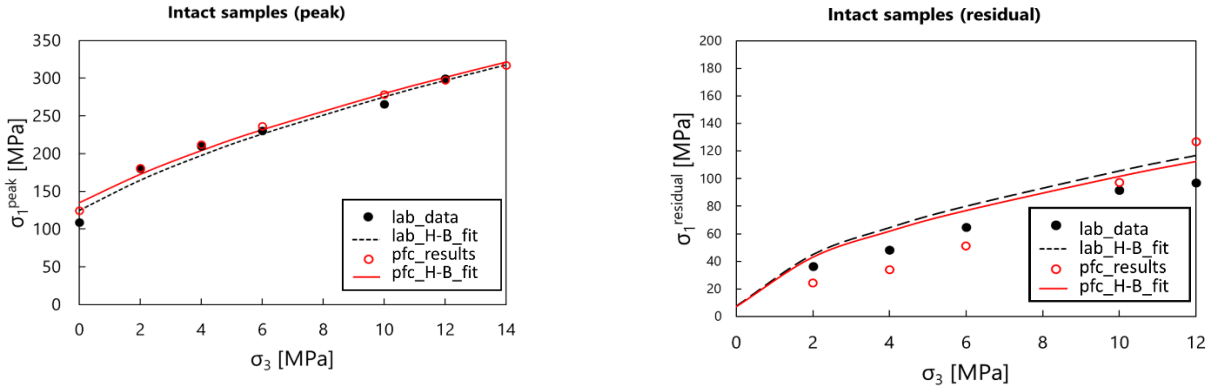

(a) (b)

Fig. 5 Representation of generalized Hoek-Brown fit for laboratory (black) and numerical simulation (red) together with the mean values for each confinement (based on Castro-Filgueira *et al.* 2020)

Table 5 Hoek-Brown parameters obtained for laboratory and PFC simulations (modified from Castro-Filgueira 2020)

H-B parameter	σ_1^{peak}		σ_1^{res}	
	Laboratory	PFC	Laboratory	PFC
m_i	43.86	40.44	43.86	40.44
σ_{ci} [MPa]	125	134.8	125	134.8
GSI	-	-	49.83	47.82
R^2	0.974	0.990	0.7052	0.7857

In order to further interpret the results, they have been analyzed with the generalized Hoek-Brown criterion, as explained in Castro-Filgueira *et al.* (2020) and in line with the lab data fitting presented above. The parameters were fitted with MATLAB software, showing the results in Table 5, together with the coefficients of determination (R^2). It should be mentioned that for the residual strength fitting, the values of σ_{ci} and m_i were fixed and derived from the corresponding intact rock results, in order to obtain comparable *GSI* values.

As observed in Fig. 5 and Table 5, both for laboratory and numerical peak strength, the fitting is relatively good, providing high coefficients of determination. When comparing H-B parameters for both data sources, the comparison is reasonably good considering the variability of the material.

In what concerns residual strength fitting, it was expected not to be as good as for peak strengths due to the more random nature of the failure process (i.e., due to differences in strain localization patterns) (Alejano *et al.* 2021).

For the case under scrutiny, the fit *GSI* values for lab and model results were quite similar, near 50, regardless of the lower values of the coefficients of determinations, compared to those for peak strength. Based on these results promising, the authors continue the research attempting to model scale effects on triaxial peak and residual intact rock strength.

4.3 Modelling of different scale specimens

A simulation plan was developed to model the results of the different size sample triaxial tests presented above. To do that, we resorted to micro-parameters calibrated in the previous study (Castro-Filgueira *et al.* 2020) and already presented in Table 3. In this study the used code was PFC6.0 instead of PFC 5.0 to run our models, in such way that the new code provides not exactly equal results, even if practically equal in average. In this context, the authors have used the micro-parameters derived from the previous study with PFC 5.0, but the original 54 mm diameter size models (Castro *et al.* 2020) were recomputed to make consistent the comparison with new data.

However, a question raises when considering appropriate PFC3D particle sizes for modelling different scale specimens: should the diameter of the particles be adapted to the specimen size or should it be kept constant?

So, in order to investigate which of these approaches could be more suitable to simulate the stress-strain behavior of different size samples, two different models were considered. In the first one, we keep constant the maximum and minimum diameter (D_{max} and D_{min}) of the particles for all specimen sizes –Case 1–, and in the second approach, we keep constant the characteristic resolution, φ_v, –Case 2–, that is, the number of grains through the relevant dimension of the specimen, i.e., its minimum dimension.

The characteristic resolution is computed as

$$\Phi_v = \frac{min(H,W,D)}{\tilde{D}_g} \tag{6}$$

Where, $\tilde{D}_g$ is the mean particle size, and *min(H,W,D)* is the minimum dimension of the discretization area, corresponding in our case to the specimen diameter. It should be mentioned that, although the characteristic resolution or diameters vary, the relation D_{max}/D_{min} keeps constant and equal to 1.66, as in previous works, because this ratio is the one that has shown to better represents a hard rock (Potyoundy and Cundall 2004). In Table 6 the particle diameters and characteristic resolutions for each specimen size and type of study are summarized.

Fig. 6 shows the particle packing of the PFC3D models of a 30 mm diameter sample for constant particle size distribution (Case 1) and for constant characteristic resolution (Case 2). As observed the number of particles considered is much smaller in the first case where the dimension of PFC3D balls has been kept constant as for the

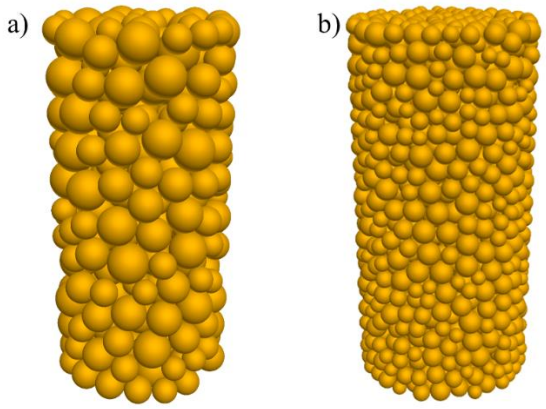

Fig. 6 Particle packings for (a) the constant size distribution approach and (b) for the constant resolution approach of a 30 mm diameter sample

Table 6 Particle diameters and characteristic resolutions for each case

Specimen radio [mm]	Case 1			Case 2		
	D_{max} [mm]	D_{min} [mm]	φ_v	D_{max} [mm]	D_{min} [mm]	φ_v
30	6.74	4.06	5.56	3.74	2.26	10
38	6.74	4.06	7.04	4.74	2.86	10
54	6.74	4.06	10	6.74	4.06	10
84	6.74	4.06	15.56	10.48	6.32	10

standard case (54 mm). In Case 2 the rough number of particles used for a 54 mm diameter intact rock sample has been kept for a 30 mm (and also for 38 and 84 mm) diameter samples, so the so-called characteristic resolution is kept constant for this modelling approach named Case 2.

Fig. 7 shows the axial stress-axial strain curve results for a 30-mm diameter sample at a confinement of 10 MPa as obtained from the lab (samples G30) and as derived from PFC3D models for constant particle size distribution (Case 1) and constant characteristic resolution (Case 2), by means of the particle assemblies presented in Fig. 6(b).

For the lab tests, the four actual lab tests carried out, including some unloading-reloading cycles, are presented. For the PFC models, the 10 model repetition results are shown for each case.

In the following subsections, the results for both approaches are presented, as well as a discussion including the Hoek-Brown failure criterion and a suggestion of future lines of the numerical study. It must be highlighted that the results for specimen size of 54 mm are the same for both modelling approaches (Case 1 and 2), due to the fact that this sample size is the one used in the previous works, corresponding to typical laboratory sample sizes.

In this case, the procedures to obtain the parameters of study were the same than for laboratory works. σ_1^{peak} was obtained as the maximum axial stress recorded. The residual strength; σ_1^{res}, was estimated as the value of the axial stress when the strength gets a value more or less constant. For all strength results (peak and residuals), mean values are presented together with the coefficient of determination for the time-consuming 560 compression-test simulations compiled in this study.

4.3.1 Packing keeping constant particle size

In the first attempt to simulate the scale effect, all specimens were assigned the same micro-properties. Taking as the starting point the simulations by Castro-Filgueira *et al.* (2020), the different size samples were modelled by keeping constant the maximum and minimum particle diameters. Considering the same diameters for the four sizes (30, 38, 54 and 84 mm) implies that the resolution characteristic in each situation varies, as shown in Table 6– Case 1.

The obtained results are shown in Fig. 8 and Table 7. In these situations, the peak strength tends to increase systematically with the specimen diameter, as Fig. 8(a) clearly depicts. Comparing these results obtained in the simulations with the laboratory ones (Tables 1 and 7), for 30 and 38 mm the increasing trend is similar for both cases – considering the natural variability of the material–, and for 84 mm peak simulations strengths are quite larger than those obtained in actual tests. The higher variability among the peak strengths can be found for the lowest confinement in the smallest specimen (30-mm tested at 0.2 MPa), something that is also true for laboratory tests.

However, for the residual strength results, the values derived from the simulations are lower than those obtained in the laboratory actual tests. Analyzing the simulation results in Fig. 8(b), a scale effect cannot be clearly identified, as it is also the case with the laboratory results. The variability of the results tends to be again higher for lower confinements and for the smaller specimens (30 and 38 mm), in line with the experimental lab residual strength results.

4.3.2 Packing keeping constant characteristic resolution

After constant resolution simulations, a new approach was chosen. Now, the characteristic resolution was varied, i.e., the particle size is adjusted to the model size. Keeping constant characteristic resolution implies that the maximum and minimum values of the particle diameters vary, as

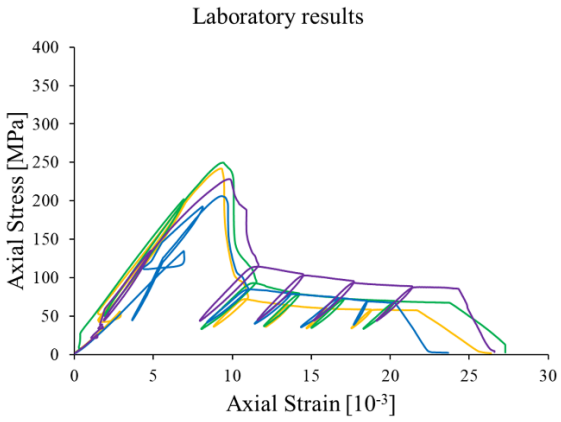

(a)

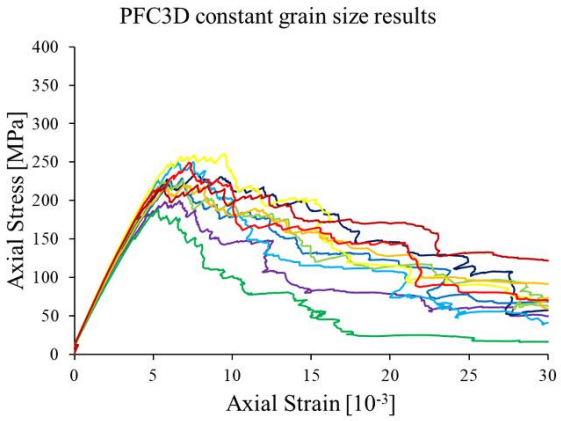

(b)

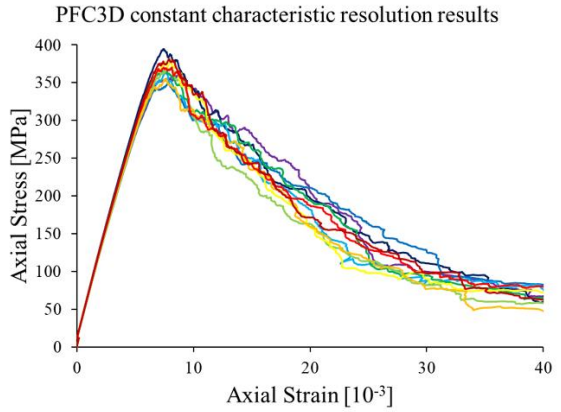

(c)

Fig. 7 Axial stress-axial strain curve for a 30 mm sample confined at 10 MPa: (a) results of 4 lab tests, (b) results of 10 numerical models for constant grain size and (c) results of 10 numerical tests for constant characteristic resolution

shown in Table 6–Case 2, increasing as the specimen diameter grows. The obtained results are shown in Fig. 9 and Table 8.

In contrast to the previous situation, the peak strength decreases with the increase of the specimen diameter, as shown in Fig. 9(a). This involves that the results for 84 mm specimens in the laboratory and simulation results are quite similar, and for 30 and 38 mm, simulations results are higher (Tables 1 and 8).

For the residual strength, although there is more variability in the results for the smallest diameters: see Fig. 9(b) and Table 8, it is lower than for the other approach. As observed when keeping constant the particle size, the results from these simulations do not show any relevant scale effect when considering the residual strength: see Fig. 9(b).

For engineering purposes, modelling keeping a constant characteristic resolution seems a good starting option, even if more research is needed to fine tune results. The authors think that more advanced contact models could facilitate PFC modelling approaches in the future.

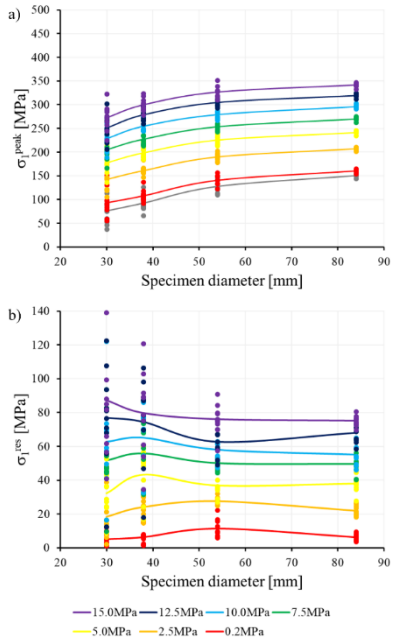

Fig. 8 Peak (a) and residual (b) strengths for different confinements and scales, considering constant the particle size

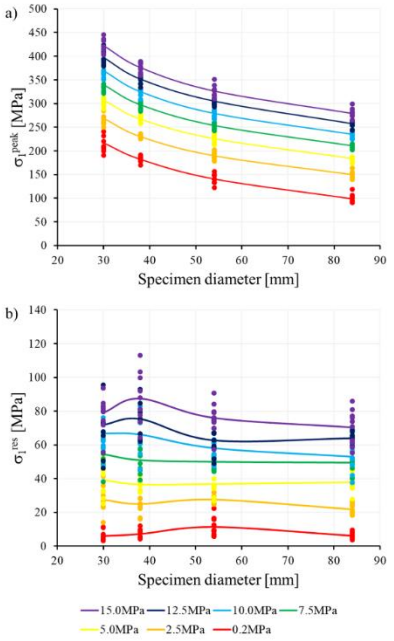

Fig. 9 Peak (a) and residual (b) strengths for different confinements and scales, considering constant the characteristic resolution

Table 7 Strength results for intact rock PFC simulations keeping constant the particle size

Specimen diameter [mm]	σ_3 [MPa]	σ_1^{peak} [MPa]		σ_1^{res} [MPa]	
		Mean.	CV [%]	Mean.	CV [%]
30	0.2	93.16	31.59	5.00	75.40
	2.5	142.14	16.47	18.42	78.09
	5.0	177.25	12.79	32.20	38.61
	7.5	205.16	10.94	51.63	44.20
	10.0	228.20	9.83	62.82	43.16
	12.5	250.73	10.94	77.05	38.89
	15.0	272.52	9.94	87.16	40.93
38	0.2	107.94	11.72	6.25	64.30
	2.5	160.78	5.89	24.16	26.38
	5.0	198.52	5.94	43.32	32.74
	7.5	227.37	5.53	55.73	25.02
	10.0	254.59	4.76	65.20	29.18
	12.5	278.84	4.50	74.55	34.40
	15.0	299.82	4.67	79.64	31.28
54	0.2	140.60	7.41	11.41	46.81
	2.5	189.84	4.18	27.63	8.03
	5.0	225.62	4.30	36.89	19.75
	7.5	253.79	3.77	50.05	10.25
	10.0	279.31	3.86	58.13	9.50
	12.5	304.99	3.40	62.81	13.24
	15.0	326.66	3.65	75.98	11.65
84	0.2	160.44	1.76	6.21	31.32
	2.5	207.07	1.28	21.96	14.01
	5.0	241.57	1.28	37.98	13.36
	7.5	270.30	1.37	49.54	14.41
	10.0	296.34	1.09	55.20	11.54
	12.5	319.64	1.18	68.13	8.36
	15.0	341.58	1.16	75.09	4.04

Table 8 Strength results for intact rocks PFC simulations keeping constant the characteristic size

Specimen diameter [mm]	σ_3 [MPa]	σ_1^{peak} [MPa]		σ_1^{res} [MPa]	
		Mean	CV [%]	Mean.	CV [%]
30	0.2	217.18	9.70	6.04	49.34
	2.5	269.20	6.52	27.54	27.82
	5.0	307.29	5.16	39.30	23.94
	7.5	340.17	4.47	54.45	13.89
	10.0	369.28	3.60	66.96	16.17
	12.5	397.06	3.56	71.92	22.16
	15.0	422.78	3.29	78.98	12.81
38	0.2	182.28	3.41	7.25	36.50
	2.5	230.31	1.70	25.10	25.37
	5.0	266.86	2.66	36.58	8.68
	7.5	297.61	2.60	51.01	20.00
	10.0	325.07	2.40	66.24	20.41
	12.5	351.50	2.70	75.40	12.78
	15.0	376.33	2.73	87.41	16.95
54	0.2	140.60	7.41	11.41	46.81
	2.5	189.84	4.18	27.63	8.03
	5.0	225.62	4.30	36.89	19.75
	7.5	253.79	3.77	50.05	10.25
	10.0	279.31	3.86	58.13	9.50
	12.5	304.99	3.40	62.81	13.24
	15.0	326.66	3.65	75.98	11.65
84	0.2	98.28	9.18	6.21	31.32
	2.5	149.77	5.09	21.96	14.01
	5.0	183.46	4.42	37.98	13.36
	7.5	210.63	3.58	49.54	14.41
	10.0	235.17	3.56	52.98	17.34
	12.5	257.19	3.53	64.04	4.48
	15.0	279.01	3.76	70.30	14.62

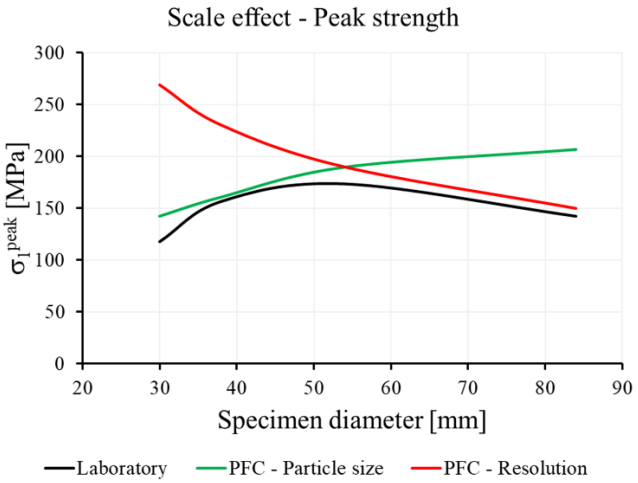

Fig. 10 Peak strength trends at 2.5 MPa confinement for laboratory and both PFC cases of study

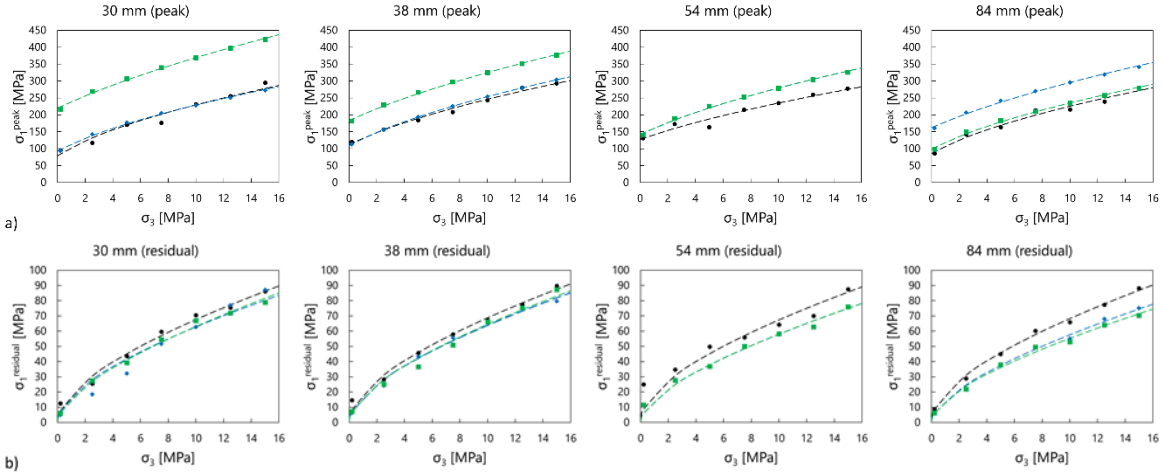

Fig. 11 Average values from laboratory (black) and simulations keeping constant the particle size (blue) and keeping constant the characteristic resolution (green) together with H-B fits for each specimen size for peak (a) and residual (b) strengths

4.3.3 Discussion

At a first sight, it seems that none of the proposed simulation approaches can represent the double scale effect observed in laboratory for the peak strength of the rock. Nevertheless, if we bring together both cases –as presented in Fig. 10 for a 2.5 MPa confinement as an example–, the double specimen size effect reported by Masoumi (2013) can be obtained. So, as a first approximation, we can suggest that the smallest specimen should be simulated keeping constant the maximum and minimum diameters of the particles, and for the larger specimens adjust these diameters to the specimen diameters, i.e., the characteristic resolution.

This effect can be better understood when fitting Hoek-Brown strength criteria to modelling and laboratory results. These fits have been obtained following the same procedure above explained for laboratory results. In Fig. 11, the Hoek-Brown fits for each specimen size, both for peak and residual strengths, are illustrated. Fit results are compiled in Table 9.

The relative lack of fit under UCS conditions can be better justified by considering the relative influence of pre-existing damage typically more relevant for unconfined tests than for confined behavior (Xu *et al.* 2018).

In Fig. 11(a) peak strength laboratory and numerical results are represented in σ_1–σ_3 axes and Hoek-Brown failure criteria surfaces are fit for each case and sample size. In Fig. 11(b) equivalent residual strength data are illustrated. In Fig. 11(a) for the smaller specimen sizes (30 and 38 mm), the H-B fit for constant diameter models (blue) are similar to the laboratory ones, something not happening for the larger diameter samples.

The results from the constant resolution diameters are the ones better representing laboratory results.

There exist proposals that could implement this type of observed size effect in the Hoek Brown criterion, as that proposed by Maosumi *et al.* (2016) for a particular sandstone. However, the implementation of this approach is not simple and should be done in an individual rock basis.

Table 9 Hoek-Brown parameters obtained from PFC simulations for each specimen size

Specimen diameter [mm]	H-B parameter	σ_1^{peak}		σ_1^{res}	
		Case 1	Case 2_v.	Case 1	Case 2_v.
30	m	42.2	36.63	42.2	36.63
	σ_{ci} [MPa]	93.04	220	93.04	220
	GSI	-	-	27.62	14.9
	R^2	0.9973	0.9965	0.9444	0.993
38	m	44.1	35.81	44.1	35.81
	σ_{ci} [MPa]	108.4	183.6	108.4	183.6
	GSI	-	-	24.05	19.03
	R^2	0.9969	0.9976	0.9929	0.9846
54	m	36.98	36.98	36.98	36.98
	σ_{ci} [MPa]	142.3	142.3	142.3	142.3
	GSI	-	-	17.96	17.96
	R^2	0.9965	0.9965	0.9805	0.9805
84	m	33.9	41.09	33.9	41.09
	σ_{ci} [MPa]	162.6	99.45	162.6	99.45
	GSI	-	-	17.24	19.83
	R^2	0.9956	0.9961	0.9948	0.992

Regarding the residual values, the generalized Hoek-Brown was fitted, in order to get the *GSI*. As shown in Fig. 11(b), the H-B fits for both simulations approaches tend to be slightly below the actual laboratory ones.

This is also reflected in the *GSI* values, which are under 28 for the simulations, and above 30 for the laboratory results. Despite these discrepancies, a clear scale effect cannot be observed in any case (both laboratory and simulations).

Based on the results presented, we hypothesize that developing models using a constant characteristic resolution could be an appropriate approach for practically simulating micromechanical processes in rock for specimens of different sizes. However, we acknowledge further research is required to establish the validity of such an approach in a definite manner.

The results obtained justify experimental test results. The presented approach used informedly provides acceptable results. Other possible approach is the potential use of Correlated Random Fields (CFR) for calibrating the micro-properties of the rock, as Le Goc *et al.* (2015) showed that CFR can reproduce the decrease of UCS of rock masses with specimen size. Other approaches in line with Haeri *et al.* (2018a, b) represent potential research lines for further study, even if more suitable for concrete than for rock. ….

5. Conclusions

Although scale effects on rock strength have been object of a good number of publications, most of these studies focused on UCS tests. Trying to further understand this effect for confined strength, the authors present a study on the scale effects on a granite for 4 different size samples (30, 38, 54 and 84 mm diameter samples) tested in lab at different confinement stresses (from 0.2 to 15 MPa).

From the laboratory results, the peak strength results present the so called double-scale effect introduced by Masoumi (2013), who reported increasing strengths from 30 to 54 mm, and then decreasing strength for higher sizes. However, residual strength results did not show any relevant scale effect.

The reason behind the observed results in simple terms, is thought to be associated to the grain size in relation to sample size. Whereas the decreasing trend of peak strength for larger samples is attributed to the so-called weak-link theory, where flaws in the sample can be found in an easier manner for larger specimens; the general although scattered inverse scale effect in smaller samples is thought to be due to effects of large grain sizes in relation to sample size.

To further study the scale effect, the laboratory tests were simulated with PFC-3D, considering two cases of study: keeping constant the maximum and minimum diameter of the particles, and keeping constant the characteristic resolution.

It is relevant to note that in this simulation approach the elastic, uniaxial and triaxial strength and post-failure response are considered for different scales, unlike in other limited scope studies where only elastic parameters or uniaxial compressive responses are accounted for in the calibration process.

For both modelling approaches, a scale effect was appreciated, but not the expected effect registered in laboratory. However, if we consider both cases together, we can get the desired effect. For smaller diameters, under NX

or 54 mm diameter the authors suggest modelling by keeping constant D_{max} and D_{min} Nevertheless, for larger diameter, above 54 mm, the authors suggest carrying out simulations by keeping constant the characteristic resolution.

From a broader rock mechanics modelling perspective, these results suggest that the correct approach for modelling typical rock problems would be that of keeping constant the characteristic resolution. This produces the typically observed and widely acknowledged effect of strength reduction with increasing size of the modelled object.

The inverse effect typical of smaller samples has only recently been identified and it is associated to particular failure modes at the scale of rock grain sizes. Although it clearly exists and it has been reported, it may not be relevant at typically larger scales normally contemplated in engineering disciplines.

In fact, the ISRM Suggested Method for uniaxial compressive testing (ISRM 2017) recommends the use of samples whose diameter is at least 10 times that of the largest grain in the rock. So according to this, and for the larger grain sizes in the range of 6 mm, samples with 30 or 38 mm will produce no reliable results.

Regarding the residual strength, relevant scale effects were neither observed for laboratory strength results nor for modelling outputs. This size-independence is consistent with recent results by other authors in different rocks and from different perspectives (Gao and Kang 2016, Walton *et al.* 2019). For the residual strength though, a rather large result variability is observed in both cases. The authors attributes this variability to the complex nature of post-failure behavior, which may produce different axial splitting zones and shear bands in the process of rock failure and different levels of interaction among them.

Acknowledgments

The authors acknowledge the Spanish Ministry of Science and Innovation for funding this study as part of the project awarded under Contract Reference No. RTI2018-093563-B-I00, partially financed by means of ERDF funds from the EU. Itasca Consulting Group is acknowledged for inviting the second author in their Itasca Education Partnership Program, which provides her with the PFC program.

References

Ajamzadeh, M.R., Sarfarazi, V., Haeri, H. and Dehghani, H. (2018), "The effect of micro parameters of PFC software on the model calibration", *Smart Struct. Syst.*, **22**(6), 643-662. https://doi.org/10.12989/sss.2018.22.6.643.

Alejano, LR., Arzúa, J., Bozorgzadeh, N. and Harrison, J P. (2017), "Triaxial strength and deformability of intact and increasingly jointed granite samples", *Int. J. Rock. Mech. Min. Sci*., **95**, 87-103. https://doi.org/10.1016/j.ijrmms.2017.03.009.

Alejano, L.R., Walton, G. and Gaines, S. (2021), "Residual strength of granitic rocks", *Tunn. Undergr. Sp. Tech*,, **118**, 104189. https://doi.org/10.1016/j.tust.2021.104189.

Arzúa, J. and Alejano, L.R. (2013), "Dilation in granite during servo-controlled triaxial strength tests", *Int. J. Rock. Mech. Min. Sci.*, **61,** 43-56. https://doi.org/10.1016/j.ijrmms.2013.02.007.

Bieniawski, Z.T. (1967), "The effect of specimen size on compressive strength of coal", *Int. J. Rock Mech. Min. Sci. Geomech. Abstr.*, **5**, 325-335. https://doi.org/10.1016/0148-9062(68)90004-1.

Brace, W.F. (1981), "The effect of size on mechanical properties of rock", *Geophys. Res. Lett.*, **8**, 651-652. https://doi.org/10.1029/GL008i007p00651.

Castro-Filgueira, U., Alejano, L.R. and Mas-Ivars, D. (2020), "Particle flow code simulation of intact and fissured granitic rock samples", *J. Rock. Mech. Geotech. Eng*., **12**, 960-974. https://doi.org/10.1016/j.jrmge.2020.01.005.

Castro-Filgueira, U., Alejano, L.R., Arzúa, J. and Mas-Ivars, D. (2016), "Numerical simulation of the stress-strain behavior of intact granite specimens with particle flow code", *Proceedings of the EUROCK 2016. International Society for Rock Mechanics (ISRM): 2016*, Cappadocia, Turkey, August.

Castro-Filgueira, U., Alejano, L.R., Arzúa, J. and Mas-Ivars, D. (2017), "Sensitivity analysis of the micro-parameters used in a PFC analysis towards the mechanical properties or rocks", *Proceedings of the EUROCK 2017. International Society for Rock Mechanics (ISRM); 2017*, Ostrava, Czech Republic, June.

Chinaei, F., Ahangari, K. and Shirinabadi, R. (2021), "Hoek-Brown failure criterion for damage analysis of tunnels subjected to blast load". *Geomech. Eng*., **26**(1), 41-47. https://doi.org/10.12989/gae.2021.26.1.041.

Cho, N., Martin, C.D. and Sego, D.C. (2007), "A clumped particle model for rock", *Int. J. Rock Mech. Min. Sci*., **44**(7), 997-1010. https://doi.org/10.1016/j.ijrmms.2007.02.002.

Coetzee, C.J. (2017), "Review: Calibration of the discrete element method". *Powder Technology* **310,** 104-142. https://doi.org/10.1016/j.powtec.2017.01.015.

Cunha, A.P. (1990), "Scale effects in rock mechanics", *Proceedings of the 1st Int. Symp. on Scale Effects in Rock Masses*, Balkema, Rotterdam, The Neederlands.

De Simone, M., Souza, L.M.S. and Roehl, D. (2019), "Estimating DEM micro-parameters for uniaxial compression simulation with genetic programming", *Int. J. Rock. Mech. Min. Sci*., **118**, 33-41. https://doi.org/10.1016/j.ijrmms.2019.03.024.

Ding, X., Zhang, L., Zhu, H. and Zhang, Q. (2014), "Effect of model scale and particle size distribution on PFC3D simulation results", *Rock Mech. Rock Eng.*, **47**(6), 2139-2156. https://doi.org/10.1007/s00603-013-0533-1.

Fan, J., Chen J., Jiang, D., Wu, J., Shu, C. and Liu, W. (2019), "A stress model reflecting the effect of the friction angle on rockbursts in coal mines", *Geomech. Eng.*, **18**(1), 21-27. https://doi.org/10.12989/gae.2019.18.1.021.

Gao, F.Q. and Kang, H.P. (2016), "Effects of pre-existing discontinuities on the residual strength of rock mass - Insight from a discrete element method simulation", *J. Struct. Geol.*, **85**, 40-50. https://doi.org/10.1016/j.jsg.2016.02.010.

Gonzalez-Fernandez, M.A., Estevez-Ventosa, X., Alonso, E. and Alejano, L.R. (2021), "Analysis of size effectss on the Hoek-Brown failure chriterion of intact granite samples", *Proceedings of the Eurock 2021 Torino. IOP Conference Series: Earth and Environmental Science*, 2021, Torino, Italy, September.

Habib, P. and Vouille, G. (1966), "Sur la disparation de l'effet d'échelle aux hautes pressions", *Compt. Rend. Hebd. des Seances de L'Acad. des Sci.*, Serie A, **262**(12), 715.

Haeri, H., Sarfarazi, V. and Zhu, Z. (2018a), "PFC3D simulation of the effect of particle size on the single edge-notched rectangle bar in bending test", *Struct. Eng. Mech*., **68**(4), 497-505. https://doi.org/10.12989/sem.2018.68.4.497.

Haeri, H., Sarfarazi, V., Zhu, Z. and Lazemi, H.A. (2018b), "Investigation of the effects of particle size and model scale on the UCS and shear strength of concrete using PFC2D", *Struct.*

Eng. Mech., **67**(5), 505-516. https://doi.org/10.12989/sem.2018.67.5.505.

Haeri, H., Sarfarazi, V., Zhu, Z., Hedayat, A. and Fatehi Marji, M. (2018c), "Investigation of the model scale and particle size effects on the point load index and tensile strength of concrete using particle flow code", *Struct. Eng. Mech*., **66**(4), 445-452. https://doi.org/10.12989/sem.2018.66.4.445.

Hazzard, J.F., Young, R.P. and Maxwell, S.C. (2000), "Micromechanical modeling of cracking and failure in brittle rocks", *J. Geophys. Res.,* **105**(7), 16683-16697. https://doi.org/10.1029/2000jb900085.

Hoek, E. and Brown, E.T. (1980), *Underground Excavations in Rock*, IMM, London, UK.

Hoek, E. and Brown, E.T. (1997), "Practical estimates of rock mass strength", *Int. J. Rock Mech. Min. Sci*., **34**, 1165-1186. https://doi.org/10.1016/S1365-1609(97)80069-X.

Hoek, E., Carranza-Torres, C. and Corkum, B. (2002), "Hoek-Brown failure criterion", *Proceedings of the NARMS-TAC 2002. Toronto, Canada: Mining Innovation and Technology*. Toronto, Canada, July.

Hoek, E., Kaiser, P.K. and Bawden, W.F. (1995), *Support of Underground Excavations in Hard Rock*, Balkena, Rotterdam, The Netherlands.

Hunt, D.D. (1973), ''The influence of confining pressure on size effect'' Ph.D. Thesis. Massachusetts Institute of Technology, Cambridge, Massachusetts.

ISRM (2007), *The Complete ISRM Suggested Methods for Rock Characterization Testing and Monitoring: 1974–2006*, Ulusay R and Hudson J, Ankara, Turkey.

Itasca (2019), *PFC 6.0 Documentation*, Itasca Consulting Group Inc, Minneapolis, MN, USA.

Kim, J., Choi, J.W., Song, J.J. (2021), "Preliminary study on PFC3D micro-parameter calibration using optimization of an artificial neural network", *Proceedings of the IOP Conference Series: Earth and Environmental Science*, **833**(1), art. no. 012096. https://doi.org/10.1088/1755-1315/833/1/012096.

Le Goc, R., Bouzeran, L., Darcel, C. and Mas-Ivars, D. (2015), "Using correlated random fields for modeling the spatial heterogeneity of rock", *Proceedings of the ISRM Regional Symposium, Eurock 2015*, Salzburg, Austria, October.

Li, K., Cheng, Y. and Fan, X. (2018), "Roles of model size and particle size distribution on macro-mechanical properties of Lac du Bonnet granite using flat-joint model", *Comput. Geotech*., **103,** 43-60. https://doi.org/10.1016/j.compgeo.2018.07.007.

Martin, D., Lu, Y., Lan, H. and Christiansson, R. (2014), "Numerical approaches for estimating the effect of scale on rock mass strength", *Proceedings of the 7th Nordic Grouting Symp.*, Gothenburg, Sweden, November.

Masoumi, H. (2013), "Investigation into the mechanical behavior of intact rock at different sizes", Ph.D. Thesis. University of New South Wales, Sydney, Australia.

Masoumi, H., Douglas, K.J., Russell, A.R., (2016), "A bounding surface plasticity model for intact rock exhibiting size-dependent behaviour". *Rock Mech. Rock Eng*., **49**(1), 47-62. https://doi.org/10.1007/s00603-015-0744-8.

Masoumi, H., Saydam, S. and Hagan, P.C. (2016), "Incorporating scale effect into a multiaxial failure criterion for intact rock", *Int. J. Rock. Mech. Min. Sci.,* **83**, 49-56. https://doi.org/10.1016/j.ijrmms.2015.12.013.

Masoumi, H., Saydam, S. and Hagan, P.C. (2015), "Unified size-effect law for intact", *Rock Int. J. Geomech.*, **16**, 04015059. https://doi.org/10.1061/(ASCE)GM.1943-5622.0000543.

Medhurst, T.P. and Brown, E.T. (1998), "A study of the mechanical behaviour of coal for pillar design", *Int. J. Rock Mech. Min. Sci.,* **35**, 1087-1105. https://doi.org/10.1016/S0148-9062(98)00168-5.

Miranda, T., Dias, D., Eclaircy-Caudron, S., Gomes Correia, A. and Costa, L. (2011), "Back analysis of geomechanical parameters by optimisation of a 3D model of an underground structure", *Tunn. Undergr. Sp. Tech*., **26**, 659-673. https://doi.org/10.1016/j.tust.2011.05.010.

Miranda, T., Correia, A.G., Santos, M., Ribeiro de Sousa, L. and Cortez, P. (2010), "New models for strength and deformability parameter calculation in rock masses using data-mining techniques", *Int. J. Geomech.*, **11**, 44-58. https://doi.org/10.1061/(ASCE)GM.1943-5622.0000071.

Obert, L. and Duvall, W.I. (1967), *Rock mechanics and the design of structures in rock*, Wiley, London, UK.

Peng, J., Wong, L.N.Y. and Teh, C.I. (2017), "Effects of grain size-to-particle size ratio on micro-cracking behavior using a bonded-particle grain-based model'', *Int. J. Rock Mech. Min. Sci.*, **100,** 207-217. https://doi.org/10.1016/j.ijrmms.2017.10.004.

Potyondy, D.O and Cundall, P.A. (2004), "A bonded-particle model for rock", *Int. J. Rock Mech. Min. Sci.*, **41**(8), 1329-1364. https://doi.org/10.1016/j.ijrmms.2004.09.011.

Potyondy, D.O. (2015), "The bonded-particle model as a tool for rock mechanics research and application: current trends and future directions", *Geosyst. Eng.*, **18**(1), 1-28. https://doi.org/10.1080/12269328.2014.998346.

Potyondy, D.O. (2018), "A flat-jointed bonded-particle model for rock", *Proceedings of the 52nd U.S. Rock Mechanics Geomechanics Symposium, American Rock Mechanics Association*, Seattle, Washington, USA, June.

Pratt, H.R., Black, A.D., Brown, W.S. and Brace, W.F. (1972), "The effect of the specimen size on the mechanical properties of unjointed diorite", *Int. J. Rock Mech. Min. Sci. Geomech. Abstr*., **9**, 513-529. https://doi.org/10.1016/0148-9062(72)90042-3.

Price, R.H. (1986), *Effects of Sample Size on the Mechanical Behavior of Topopah Spring Tuff*, Sandia National Laboratories, Albuquerque, NM, USA.

Quiñones, J., Arzúa, J., Alejano, L.R., García-Bastante, F., Mas-Ivars, D. and Walton, G. (2017), "Analysis of size effects on the geomechanical parameters of intact granite samples under unconfined conditions", *Act. Geotech.*, **12**(6), 1229-1242. https://doi.org/10.1007/s11440-017-0531-7.

Ranjbarnia, M., Rahimpour, N. and Oreste, P. (2020), "A new analytical-numerical solution to analyze a circular tunnel using 3D Hoek-Brown failure criterion", *Geomech. Eng*., **22(**1), 11-23. https://doi.org/10.12989/gae.2020.22.1.011.

Schöpfer, M., Abe, P.J., Childs, C. and Walsh, J.J. (2009), "The impact of porosity and crack density on the elasticity, strength and friction of cohesive granular materials: insight from DEM modelling", *Int. J. Rock Mech. Min. Sci*., **46**(2), 250-261. https://doi.org/10.1016/j.ijrmms.2008.03.009.

Tuncay, E. and Hasancebi, N. (2009), "The effect of length to diameter ratio of test specimens on the uniaxial compressive strength of rock", *Bull. Eng. Geol. Environ*., **68**, 491-497. https://doi.org/10.1007/s10064-009-0227-9.

Walton, G. (2018), "Scale effects observed in compression testing of stanstead granite including post-peak strength and dilatancy", *Geotech. Geol. Eng.*, **36**(2), 1091-1111. https://doi.org/10.1007/s10706-017-0377-7.

Walton, G., Labrie, D. and Alejano, LR. (2019), "On the residual strength of rocks and rockmasses", *Rock Mech. Rock Eng*., **52**, 4821-4833. https://doi.org/ 10.1007/s00603-019-01879-5.

Weibull, W. (1939), "A statistical theory of the strength of materials", *Proceedings of the Royal Swedish Acad. of Eng. Science*, Stockholm, Sweden.

Wu, S. and Xu, X. (2016), "A study of three intrinsic problems of the classic discrete element method using flat-joint model", *J. Rock Mech. Rock Eng.*, **49**, 1813-1830. https://doi.org/10.1007/s00603-015-0890-z.

Xu, Z., Li, T., Chen, G., Ma, C., Qiu, S. and Li, Z. (2018), "The grain-based model numerical simulation of unconfined

compressive strength experiment under thermal-mechanical coupling effect", *KSCE J. Civil Eng.*, **22**, 2764-2775. https://doi.org/10.1007/s12205-017-1228-z.

Xu, Z.H., Wang, W.Y., Lin., P, Xiong, Y., Liu, Z.Y. and He, S.J. (2020), "A parameter calibration method for PFC simulation: Development and a case study of limestone", *Geomech. Eng.*, **22**(1), 97-108. https://doi.org/10.12989/gae.2020.22.1.097.

Xu, C., Liu, X., Wang, E. and Wang, S. (2021), "Calibration of the micro-parameters of rock specimens by using various machine learning algorithms", *Int. J. Geomech.*, **21**, 04021060. https://doi.org/10.1061/(ASCE)GM.1943-5622.0001977.

Yang, S.Q., Tian, W.L., Jing, H.W., Huang, Y.H., Yang, X.X. and Meng, B. (2019), "Deformation and damage failure behavior of mudstone specimens under single-stage and multi-stage trialxial compression", *Rock Mech. Rock Eng.*, **52**(3), 673-689. https://doi.org/ 10.1007/s00603-018-1622-y.

Yoon, J. (2007), "Application of experimental design and optimization to PFC model calibration in uniaxial compression simulation" *Int. J. Rock Mech. & Min. Sci.* **44**(6), 871-889. https://doi.org/10.1016/j.ijrmms.2007.01.004.

Yoshinaka, R., Osada, M., Park, H., Sasaki, T. and Sasaki, K. (2008), "Practical determination of mechanical design parameters of intact rock considering scale effect", *Eng. Geol.*, **96**(3-4), 173-186. https://doi.org/10.1016/j.enggeo.2007.10.008.

Zhou, C., Xu, C., Karakus, M. and Shen, J. (2018), "A systematic approach to the calibration of micro-parameters for the flat-jointed bonded particle model". *Geomech. Eng.*, **16**(5), 471-482. https://doi.org/10.12989/gae.2018.16.5.471.

CC